Formation pathways of proteins in space

Sergiy Krasnokutskiy (sergiy.krasnokutskiy@uni-jena.de)
Laboratory Astrophysics Group of the Max Planck Institute for Astronomy at the University of Jena
https://orcid.org/0000-0002-9816-3187

Ko-Ju Chuang
Laboratory Astrophysics Group of the Max Planck Institute for Astronomy at the University of Jena

Cornelia Jaeger
Max Planck Institute for Astronomy and Friedrich Schiller University Jena https://orcid.org/0000-0001-7803-0013

Nico Ueberschaar
Mass Spectrometry Platform, Faculty of Chemistry and Earth Sciences, Friedrich Schiller University Jena

Thomas Henning
MPI for Astronomy https://orcid.org/0000-0002-1493-300X

Article

Keywords: Prebiotic Molecules, Space Conditions, Atomic Carbon Condensation, Monomeric Fragments of Polyglycine, Polypeptides, Origin of Life

Posted Date: February 23rd, 2021

DOI: https://doi.org/10.21203/rs.3.rs-238307/v1

Formation pathways of proteins in space

S.A. Krasnokutski[1*], K.-J. Chuang[1†], C. Jäger[1], N. Ueberschaar[2], and T. Henning[3]

[1]Laboratory Astrophysics Group of the Max Planck Institute for Astronomy at the Friedrich Schiller University Jena, Helmholtzweg 3, D-07743 Jena, Germany. *Email: sergiy.krasnokutskiy@uni-jena.de

[2]Mass Spectrometry Platform, Faculty of Chemistry and Earth Sciences, Friedrich Schiller University Jena, Humboldstr. 8, 07743 Jena, Germany.

[3]Max Planck Institute for Astronomy, Königstuhl 17, 69117 Heidelberg, Germany.

†Current address: Leiden Observatory, Leiden University, P.O. Box 9513, NL–2300 RA Leiden, The Netherlands.

Until now, experiments demonstrated the possible formation of relatively small prebiotic molecules under typical space conditions. We demonstrated experimentally that condensation of atomic carbon on the surface of cold solid particles (cosmic dust) leads to the formation of monomeric fragments of polyglycine. These fragments polymerize effectively producing polypeptides. The chemistry involves three of the most common species (CO, C, and NH_3) present in star-forming molecular clouds. It proceeds via a novel pathway that skips the stage of amino acids formation in protein synthesis and is effective even at low temperatures without irradiation or presence of water. Therefore, the amount of proteins formed in space through this process could be quite substantial. The delivery of proteins to rocky planets in the habitable zone might be an important element for the origin of life.

The origin of life has always been one of the most intriguing questions throughout human history. Biomolecules delivered to early Earth by asteroids or comets during the period of heavy bombardment about four billion years ago have been proposed to play a role in the origin of life [1,2]. Similar processes may apply to rocky exoplanets. Analysis of meteoritic materials led to the identification of amino acids, sugars, and nucleobases, among other complex organic molecules of extraterrestrial origin [3]. The amino acid glycine has been discovered in comets [4]. The widely accepted hypothesis of the formation of organic molecules in space assumes their synthesis in ice mantels covering the refractory dust grains present in space [5]. At later stages when asteroids are formed from this dust, the chemistry in liquid water may also enhance the molecular complexity [6]. Experimentally, the formation of a variety of amino acids, and even their dimers as well as other organic molecules, was detected after energetic processing of different molecular ices [7,8]. These experiments are comparable to Urey-Miller-type experiments performed at elevated temperatures [9]. The non-energetic pathway was also found for different small organic molecules [10,11] and even glycine [12,13]. However, till now, only very small fragments of biopolymers were found to be formed in these experiments.

The formation of peptides and proteins is usually considered as a polymerization process of amino acids. This process requires the condensation of amino acids accompanied by the loss of water. This is a thermodynamically unfavourable process and, therefore, it proceeds at high temperatures under the assistance of catalysts or requires energetic processing of the material [14]. Therefore, the prebiotic synthesis of peptides is thought to occur in two steps, each of which has a low probability [15]. Instead of first synthesizing amino acids in order to subsequently break them down for the polymerization process, we suggest a very efficient and direct formation of the monomeric fragments of peptides and its further polymerization. This reaction between NH_3, C,

and CO occurs on the cold dust grains, without external energy. Quantum chemical calculations predict that the CO + C + NH_3 $\xrightarrow{surface}$ NH_2CH=CO reaction is barrierless [16]. The polymerization of NH_2CH=CO results in the formation of peptide chains. In contrast to the polymerization of the amino acids, the polymerization of NH_2CH=CO is a much simpler process.

To test this reaction pathway experimentally, we performed co-deposition of these species on the surface of both Si and KBr substrates cooled to 10K and placed inside an ultra-high vacuum (UHV) chamber. Low-energy carbon atoms were generated by a dedicated atomic carbon source [17]. The background pressure inside the vacuum chamber (1×10^{-10} mbar) and the temperature of the substrate (10 K) allowed us to mimic dense molecular cloud conditions.

Low-temperature chemistry, *T* = 10 K

Infrared absorption spectra of the ice produced after the co-deposition of CO + NH_3 and CO + C + NH_3 are shown in Figure 1. The addition of C atoms during the deposition leads to the appearance of new absorption peaks. The control experiments involving only two reactants C + CO and C + NH_3 are given in the supplementary materials (see Figures S1, S2, S3).

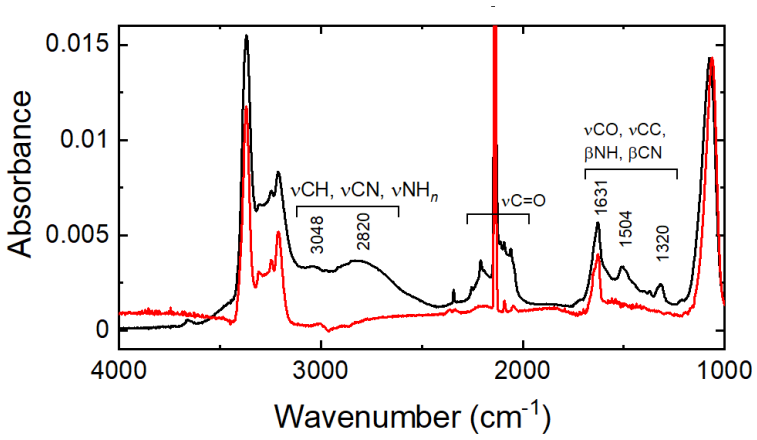

Figure 1. IR absorption spectra of the material produced by co-deposition of CO + NH_3 (red) and CO + C + NH_3 (black).

The deposition of all three reactants (CO, C, NH_3) on the substrate at 10 K reveals new IR absorption bands, which were not observed in any experiment involving only two reactants. Therefore, these bands have to be assigned to a product formed by all three reactants. Moreover, we observed only negligible amounts of the residue at 300 K in the experiments involving only two reactants. Thus, we conclude that during the deposition at 10 K, the reaction involves all three reactants, and exactly the product of this reaction is required for the formation of the non-volatile products at 300 K.

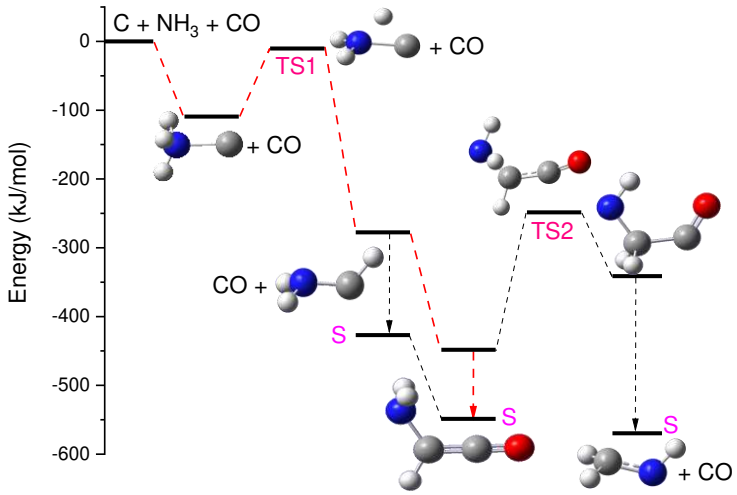

Figure 2. Energy level diagram for the reaction involving CO, C, and NH_3 reactants. The reaction starts with the triplet state. The transition states and the singlet states are marked with TS and S, respectively. The dashed lines show the possible reaction pathways and the red colour marks the most probable one.

To better understand the chemistry of all three reactants at 10K, we performed quantum-chemical calculations. Their results are shown in Figure 2. The C atom initially prefers to react with the ammonia molecule. The pathway of this reaction was studied experimentally [13] using the recently developed calorimetric technique [18]. The overcome of the first transition state was confirmed. The NH_2CH reacts barrierlessly with CO leading to the formation of $NH_2CH{=}CO$. Therefore, there are two most possible products of this reaction - $NH_2CH{=}CO$ and (CH_2NH +

CO). The last one is the same as the product of the reaction C + NH_3. Therefore, the reaction of three reactants results in the formation of the NH_2CH=CO product at 10 K. The formation of this molecule is also confirmed later during the temperature-programmed desorption (TPD) by monitoring the ions with the masses of 57 and 56 u (see Figure S4). At the same time, a number of C atoms could react with either CO or NH_3 only. It could lead to the formation of some number of CCO as well as H_2CNH and $NH_2CH_2NH_2$ molecules.

Chemical transformation during temperature rise

After the deposition, the substrate was heated with a rate of 2 K per min. The IR spectra measured at important temperatures are shown in Figure 3.

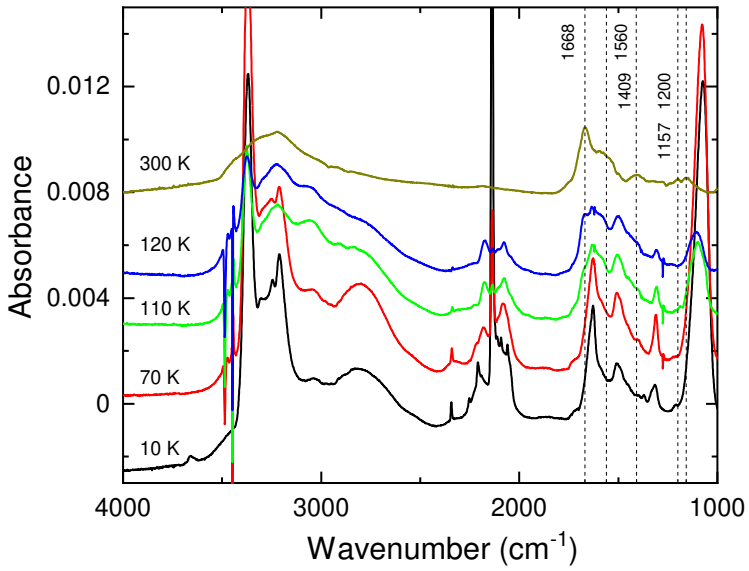

Figure 3. IR absorption spectra during the annealing of the material produced by co-deposition of CO + C + NH_3. Vertical numbers show the positions of the peaks appearing during heating, while horizontal ones displays the temperature of the substrate.

The comparison of the spectra at 10 K and 70 K shows that the evaporation of carbon monoxide, started at about 30 K, does not initiate a new chemistry. However, with evaporation of ammonia, the products of the C atom reactions can finally meet each other and react. We observed the formation and growth of new IR absorption bands 1668, 1560, while the intensity of the νNH_n

bands νC=O bands decreased significantly. With the mass spectrometer we did not detect any considerable desorption from the substrate besides CO and NH_3 gases. Therefore, the disappearance of the IR bands is rather due to the chemical transformation than the evaporation of the corresponding material. The decrease in the intensity of bands in the 2800 – 3050 cm^{-1} range is a common indication of the glycine polymerization [19]. This takes place because the NH_3^+ or NH_2 groups of glycine are transformed into NH groups present in peptides. Additionally, the C=O stretching vibration in $NH_2CH=CO$ disappears and we observe the formation of the amide I band at 1668 cm^{-1} CO stretching and amide II at 1560 cm^{-1}, which are characteristic for the peptide bond. After complete ammonia evaporation, no considerable changes in the IR spectra were observed. Therefore, the material present on the substrate after warming up to 300 K (R300K) should have been formed at low temperature during ammonia evaporation.

Characterization of the room temperature residue

The characterization of R300K was performed using both in situ FTIR spectroscopy and ex situ high-resolution mass spectrometry. Due to a very high resolution, the mass spectrometry provides exact data on elemental compositions of molecules in the low and middle mass ranges, while the IR spectroscopy shows the type of bonds present in these molecules. Analysis of these experimental data in combination with the information about the molecules formed at T = 10 K, allows us to draw the conclusions about the R300K material.

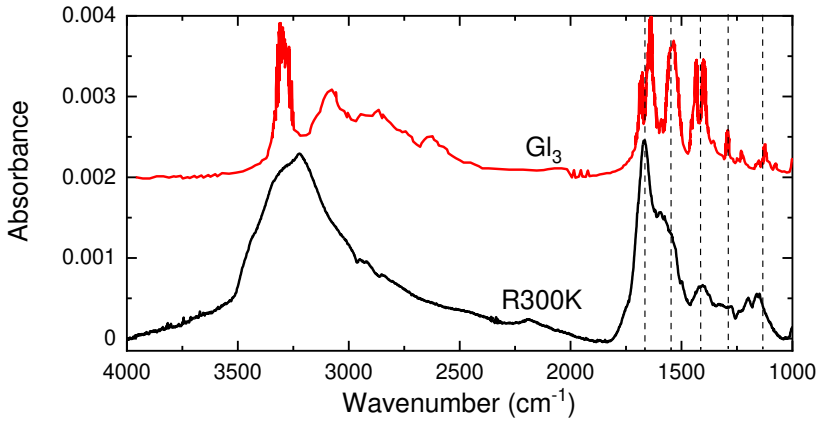

Figure 4. Comparison of the IR absorption spectra of R300K and triglycine (Gl_3) adopted from ref 20. The vertical dashed lines are drawn to visualize the coincidences between the peaks in two spectra.

The IR spectrum of R300K is shown in Figure 4. It highlights the absorption features characteristic for the peptide bond. As can be seen, the spectra of R300K resemble the spectra of the glycine peptide quite closely. The main difference is a much higher width of absorption bands observed in the spectra of the R300K. This broadening is assigned to the formation of peptide chains of different lengths, which is also detected by the mass spectrometry, which we present later. It has been shown that the IR absorption band positions and intensities change notably with the number of units in the glycine oligomers [20]. Moreover, the molecular structure of the peptide terminal groups formed in our experiments is not completely known. The polymerization of $NH_2CH{=}CO$ molecules with the formation of peptide chains requires the proton transfer from nitrogen to the carbon atom of the CH group. At the same time, our DFT calculations show that $NHCH_2CO$ as well as $NH_2CHCO\text{-}NHCH_2CO$ molecules are not stable. They fragment by abstraction of the CO molecule. Therefore, the calculations predict that the peptide chains produced by this mechanism are terminated by NH_2 on one side, which corresponds to the classical structure of the peptide. On the other peptide side, instead of having

a classical COOH group, it is terminated by the CH_2 group. This should also affect the IR spectra in particular in the case of short chains.

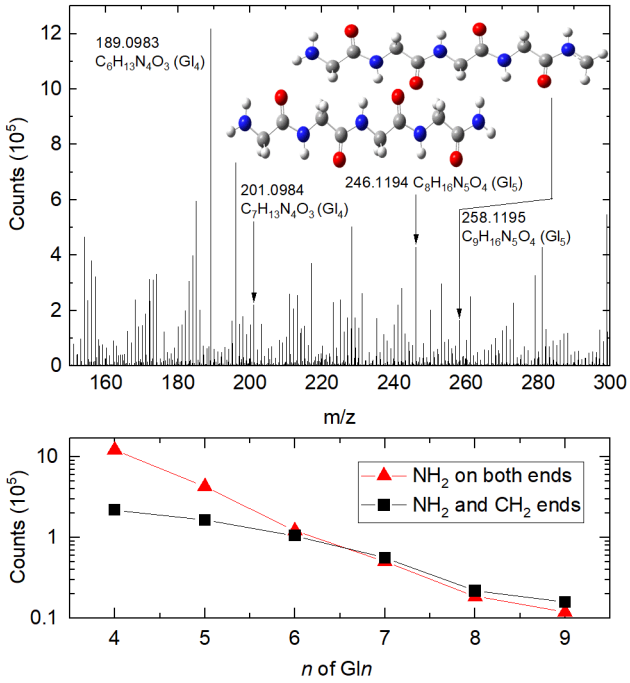

Figure 5. The mass spectra of the 300 K residue obtained from ex situ analysis using ESI-Orbitrap mass spectrometer. The molecular structures displayed resemble the Gl_5 peptides detected in the mass spectra as protonated species $[analyte+H]^+$. In the lower frame, the intensities of the bands from mass spectrum corresponding to the glycine peptides are plotted as a function of the peptide length.

Ex situ mass spectrum of R300K is shown in Figure 5. We could identify a series of mass peaks, which corresponds to the theoretically expected structures of the peptides terminated by NH_2 and CH_2 groups starting from the glycine tetramer up to the glycine nonamer. The peaks are separated by the mass of 57.0215 u. This value exactly matches the mass of the $NH_2CH{=}CO$ molecule, which was also detected by in situ mass spectrometry. However, the observed series is not the most intense one. The most intense peak (189.0983 u) in the mass spectrum belongs to the glycine tetramer terminated on both sides with NH_2 groups. We can also identify the series of mass peaks corresponding to such a structure up to the glycine nonamer, and other series of mass peaks separated always by 57.0215 u. For example, the series that exactly corresponds to the

masses of the $(NH_2CHCO)_n$ molecules as well as the NH_2/NH_2 terminated peptides with addition of C_2, H_2, and C_3H were detected. The complete list of all found series is given in the supplementary materials. The formation of a variety of different peptides can be understood assuming that the oligomerized NH_2CHCO molecules contain reactive sites. In the expected dimer $NH_2CHCO\text{-}NHCH_2$, the C atoms in CH and CH_2 groups are not saturated and could join other species. Therefore, other products formed at 10 K could be added during the polymer formation. More complex chemistry could take place during the solvation. However, as most of main peaks in the mass spectrum belong to the series, where peaks are separated by 57.0215 u, we conclude that the polymerization of the $NH_2CH{=}CO$ molecule is the main chemical pathway in our experiment.

The polymerization of $NH_2CH{=}CO$ requires the nucleophilic attack of the nitrogen on the carbonyl carbon and an intramolecular proton transfer from NH_2 to CH. Our DFT computations show a large barrier of about 240 KJ mol^{-1} for the proton transfer from NH_2 to the CH group in the isolated $NH_2CH{=}CO$ molecule. Therefore, the polymerization is expected to take place either with the action of a catalyst, which could be ammonia molecules, or by proton transfer via tunnelling. The tunnelling could be quite efficient due to the quantum nature of the proton motion. Even at room temperatures, the role of the tunnelling was found to be significant in a variety of intramolecular proton transfer reactions [21]. The efficient polymerization of the $NH_2CH{=}CO$ molecule at low temperatures is in line with the fact that this molecule, to the best of our knowledge, has never been observed in experimental studies. As the isolated molecule is predicted to be stable, their non-detection in previous experiments should be assigned to a high reactivity of this molecule.

Implications

The reactants used in the current study are among the most abundant species present in the interstellar medium (ISM). The fractional abundance of NH_3 and CO in the ice mantels covering refractory dust particles amounts to up 10% and 40%, respectively [22]. More than 50% of all carbon in the ISM exist in the form of atomic gas [23]. Therefore, reactions between CO, C, and NH_3 could be very common. This is a static point of view. In dynamic terms, the reactions of C atoms become even more important. The carbonaceous stardust is expelled in the ISM by dying starts. In the ISM, the stardust is atomized by shockwaves of supernova explosions [24-26]. Therefore, the dust, from which planets, asteroids, and comets will be formed at later stages, has to be formed in the ISM due to the accretion of gaseous species. The C atoms could be converted to the molecular form before the accretion. However, this is a relatively long process[27]. Therefore, a notable portion of carbonaceous dust is expected to be formed by the accretion of C atoms. This leads to the formation of organics [28]. As revealed by the current study, a notable portion of this organics could be in the form of peptides. This dust becomes building blocks of comets or meteorites. Therefore, the formed organics can be delivered to early Earth during the period of a heavy bombardment. An important issue is the stability of the formed organics and whether it can be delivered to planets. In this matter, the spontaneous - non energetic way of the peptide formation is a big advantage. If gas to solid phase transition occurs in the ISM in the areas of a low UV flux, the formed proteins can survive long enough and finally be incorporated into bulk solids, which would protect them. The fact that they can survive and be delivered to planets is demonstrated by two very recent publications showing the presence of proteins in meteorites [29,30]. Proteins and organics can be preserved even better in most pristine and unprocessed material present in comets. They might deliver intact organics produced in the ISM at a rate of at least 10^6 to 10^7 kilograms per year [2]. At the same time, peptides play a key role in

196 the origin of life [15]. Therefore, the delivery of proteins to Earth should expand the opportunities
197 for the origin of life. Thus, the conditions, under which the origin of life was commonly
198 considered to be possible, should be revised. A large variety of peptides formed in this way could
199 considerably increase a chance that the molecules required for the chemistry leading to
200 abiogenesis will be formed. Therefore, the low-temperature chemistry that happens between the
201 stars could go a long way towards the origin of life on Earth and exoplanets.

202 **Methods**

203 **In situ experiments.** The experiments were performed using the ultrahigh vacuum (UHV) setup,
204 INterStellar Ice Dust Experiment (INSIDE), described elsewhere [31]. We performed co-deposition
205 of CO, C, and NH_3 reactants on the surface of KBr substrates cooled to 10K and placed inside an
206 ultra-high vacuum (UHV) chamber. The deposition of reactants was performed for about one
207 hour. Low-energy carbon atoms were generated by an atomic carbon source [17]. The source
208 generates pure flux of low-energy carbon atoms in the triplet ground state $C(^3P_J)$. The
209 background pressure inside the vacuum chamber (1×10^{-10} mbar) and the temperature of the
210 substrate (10 K) allowed us to mimic dense molecular cloud conditions. We used about equal
211 amounts of CO and NH_3 molecules, while the number of C atoms was at least ten times smaller.
212 This small amount of C atoms allows to exclude their reactions with each other as well as with
213 their reaction products. The gases were introduced through two separated gas lines. The ice
214 thicknesses on substrates were monitored by infrared (IR) spectroscopy. IR spectra were
215 measured using an FTIR spectrometer (Vertex 80v, Bruker) in the transmission mode. In situ
216 mass spectra were measured by a quadrupole mass spectrometer (HXT300M, Hositrad) located
217 in the same UHV chamber. After the deposition, the substrate was heated with a rate of 2 K per
218 min. During the warming up process of the material, the IR absorption spectra of the deposit as

well as the mass spectra of the species released to the gas phase were measured. The TPD curves were obtained by integrating the area of the corresponding bands in the IR and mass spectra.

Ex situ mass spectrometry analysis. For the mass spectrometry analysis, we used silicon substrates and performed a 4-hours deposition of CO, C, and NH_3 reactants at the same conditions as in the in situ experiments. We obtained very similar IR spectra on all stages of the experiment, using both Si and KBr substrates. The main difference in the IR spectra of these two substrates was the appearance of Si absorption features during the TPD. Therefore, they were not used for in situ analysis. After warming up, the substrates were left overnight in the UHV chamber, after which they were removed and analysed. The residue was extracted with a water/methanol mixture (70/30) and provided for the mass spectral analysis. The mass spectrometry was performed using the hybrid linear trap/Orbitrap mass spectrometer (Thermo fisher QExactive plus mass spectrometer with a heated ESI source). The accuracy of the mass determination is higher than 5 ppm, which, for the investigated mass range, means a possible error only in the fourth decimal place. Considering the limited number of elements used in the experiments (C, O, N, and H), this high resolution allows to define unambiguously the elemental composition of the detected ions in the mass range shown in Figure 5. To ensure that the observed mass peaks are due to the material formed in our experiment, the possible presence of contaminants both on the substrate and in the mass spectrometer were checked using the same procedure with clean silicon substrates.

Quantum-chemical computations. Molecular geometries of the reactants and products of chemical reactions were determined at B3LYP/6-311+G (d,p) level as implemented in the GAUSSIAN16 [32]. The reaction energies were found as the difference between the sum of the energies of reactants and the energy of the product molecules with vibrational zero-point energy

corrections. The two dimensional potential energy scan of the CO + C + NH_3 reaction was performed at MP2/6-311+G (d, p) level.

Data availability. The data that support the plots within this paper and other findings of this study are available from the corresponding author upon reasonable request.

References

1 Pearce, B. K. D., Pudritz, R. E., Semenov, D. A. & Henning, T. K. Origin of the RNA world: The fate of nucleobases in warm little ponds. *Proc. Natl. Acad. Sci. U.S.A.* **114**, 11327-11332, (2017).

2 Chyba, C., Thomas, P., Brookshaw, L. & Sagan, C. Cometary delivery of organic molecules to the early Earth. *Science* **249**, 366-373, (1990).

3 Pizzarello, S. & Cronin, J. R. Alanine enantiomers in the Murchison meteorite. *Nature* **394**, 236-236, (1998).

4 Altwegg, K. *et al.* Prebiotic chemicals—amino acid and phosphorus—in the coma of comet 67P/Churyumov-Gerasimenko. *Sci. Adv.* **2**, e1600285, (2016).

5 Herbst, E. & van Dishoeck, E. F. Complex Organic Interstellar Molecules. *Annu. Rev. Astron. Astrophys.* **47**, 427-480, (2009).

6 Abramov, O. & Mojzsis, S. J. Abodes for life in carbonaceous asteroids? *Icarus* **213**, 273-279, (2011).

7 Kaiser, R. I., Stockton, A. M., Kim, Y. S., Jensen, E. C. & Mathies, R. A. On the Formation of Dipeptides in Interstellar Model Ices. *Astrophys. J.* **765**, (2013).

8 Caro, G. M. M. *et al.* Amino acids from ultraviolet irradiation of interstellar ice analogues. *Nature* **416**, 403-406, (2002).

9 Miller, S. L. A Production of Amino Acids Under Possible Primitive Earth Conditions. *Science* **117**, 528, (1953).

10 Potapov, A., Jäger, C., Henning, T., Jonusas, M. & Krim, L. The Formation of Formaldehyde on Interstellar Carbonaceous Grain Analogs by O/H Atom Addition. *Astrophys. J.* **846**, 131, (2017).

11 Chuang, K.-J. *et al.* Production of complex organic molecules:H-atom addition versus UV irradiation. *Mon. Not. R. Astron. Soc.* **467**, 2552-2565, (2017).

12 Ioppolo, S. *et al.* A non-energetic mechanism for glycine formation in the interstellar medium. *Nat. Astron.*, (2020).

13 Krasnokutski, S. A., Jäger, C. & Henning, T. Condensation of Atomic Carbon: Possible Routes toward Glycine. *Astrophys. J.* **889**, 67, (2020).

14 Kitadai, N. & Maruyama, S. Origins of building blocks of life: A review. *Geosci. Front.* **9**, 1117-1153, (2018).

15 Frenkel-Pinter, M., Samanta, M., Ashkenasy, G. & Leman, L. J. Prebiotic Peptides: Molecular Hubs in the Origin of Life. *Chem. Rev.* **120**, 4707-4765, (2020).

16 Krasnokutski, S. A. Did life originate from low-temperature areas of the Universe? *Fiz. Nizk. Temp.* **47**, 219–226, (2021).

17 Krasnokutski, S. A. & Huisken, F. A simple and clean source of low-energy atomic carbon. *Appl. Phys. Lett.* **105**, 113506, (2014).

18 Henning, T. K. & Krasnokutski, S. A. Experimental characterization of the energetics of low-temperature surface reactions. *Nat. Astron.* **3**, 568-573, (2019).
19 Ali, M. F. B. & Abdel-aal, F. A. M. In situ polymerization and FT-IR characterization of poly-glycine on pencil graphite electrode for sensitive determination of anti-emetic drug, granisetron in injections and human plasma. *RSC Advances* **9**, 4325-4335, (2019).
20 Taga, K. *et al.* FT-IR spectra of glycine oligomers. *Vib. Spectrosc* **14**, 143-146, (1997).
21 Jose, D. & Datta, A. Tunneling Governs Intramolecular Proton Transfer in Thiotropolone at Room Temperature. *Angew. Chem. Int. Ed.* **51**, 9389-9392, (2012).
22 Oberg, K. I. Photochemistry and Astrochemistry: Photochemical Pathways to Interstellar Complex Organic Molecules. *Chem. Rev.* **116**, 9631-9663, (2016).
23 Snow, T. P. & Witt, A. N. The Interstellar Carbon Budget and the Role of Carbon in Dust and Large Molecules. *Science* **270**, 1455-1460, (1995).
24 Draine, B. T. Inrestellar dust models and evolutionary implications. *Cosmic dust - near and far, ASP Conference Series, ed. Th. Henning, E. Grün, and J. Steinacker* **414**, 453, (2009).
25 Jones, A. P. & Nuth, J. A. Dust destruction in the ISM: a re-evaluation of dust lifetimes. *Astron. Astrophys.* **530**, A44, (2011).
26 Zhukovska, S. Dust origin in late-type dwarf galaxies: ISM growth vs. type II supernovae. *Astron. Astrophys.* **562**, A76, (2014).
27 Phillips, T. G. & Huggins, P. J. Abundance of Atomic Carbon (C-1) in Dense Inter-Stellar Clouds. *Astrophys. J.* **251**, 533-540, (1981).
28 Krasnokutski, S. A. *et al.* Low-temperature Condensation of Carbon. *Astrophys. J.* **847**, 89, (2017).
29 Lange, J. *et al.* A Novel Proteomics-Based Strategy for the Investigation of Peptide Sequences in Extraterrestrial Samples. *J. Proteome Res.*, (2020).
30 McGeoch, M. W., Dikler, S. & McGeoch, J. E. M. Hemolithin: a Meteoritic Protein containing Iron and Lithium. (https://arxiv.org/abs/2002.11688).
31 Potapov, A., Theule, P., Jager, C. & Henning, T. Evidence of Surface Catalytic Effect on Cosmic Dust Grain Analogs: The Ammonia and Carbon Dioxide Surface Reaction. *Astrophys. J. Lett.* **878**, L20, (2019).
32 Frisch, M. J., *et. al.* Gaussian 16 Rev. C.01 (Wallingford, CT, 2016).

Acknowledgements

This work was financially supported by the Max Planck Institute for Astronomy (MPIA). S.K. acknowledges support from Deutsche Forschungsgemeinschaft DFG (grant No. KR 3995/4-1). T.H. acknowledges support from the European Research Council under the Horizon 2020 Framework Program via the ERC Advanced Grant Origins 83 24 28.

Author contributions

S.K. initiated and led the project, S.K. and K.J.C. recorded and analysed the experimental data. S.K. performed the computations and wrote the manuscript. N.U. performed ex situ mass spectrometry. T.H. and C.J. participated in data interpretation and discussion. All authors contributed to the writing of the manuscript.

Competing interests

The authors declare no conflict of interest.

Figures

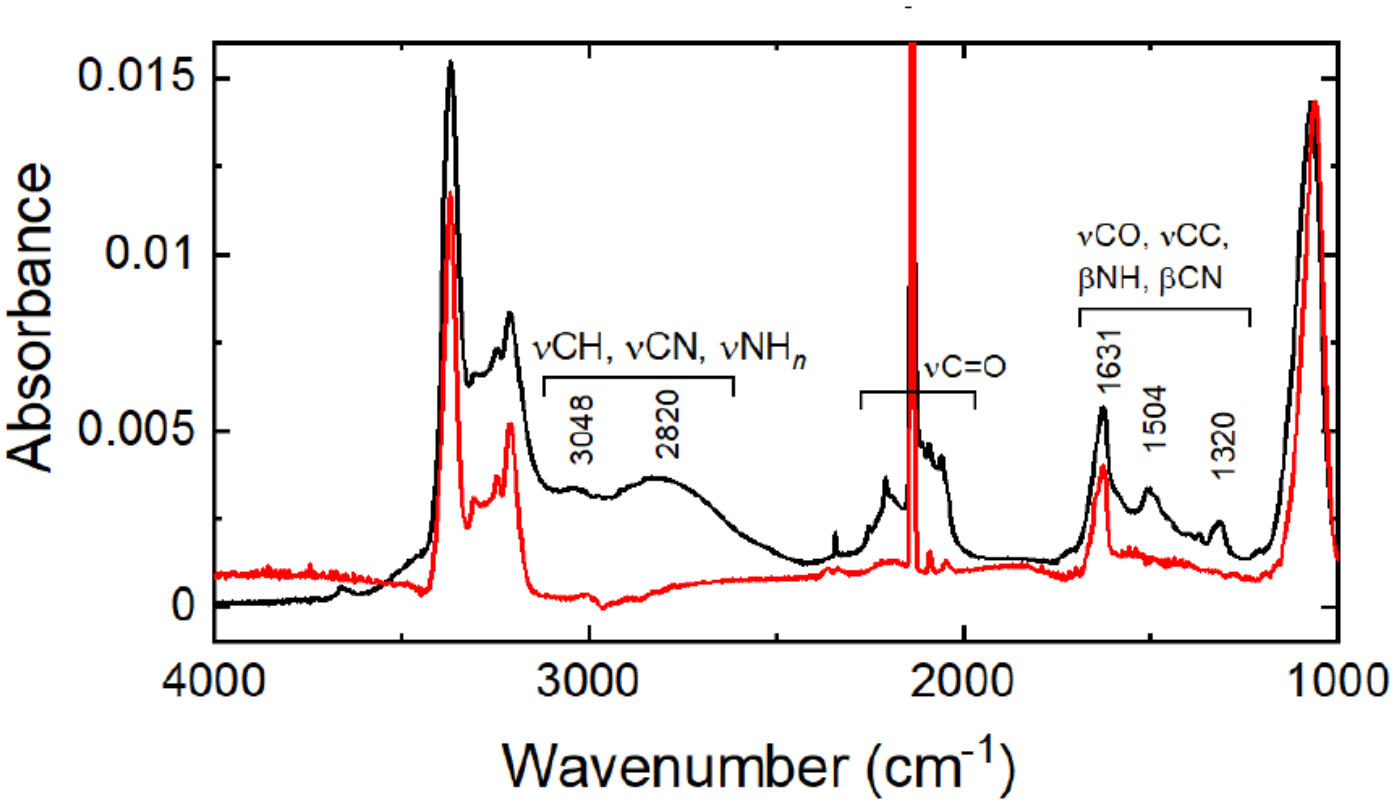

Figure 1

IR absorption spectra of the material produced by co-deposition of CO + NH3 (red) and CO + C + NH3 (black).

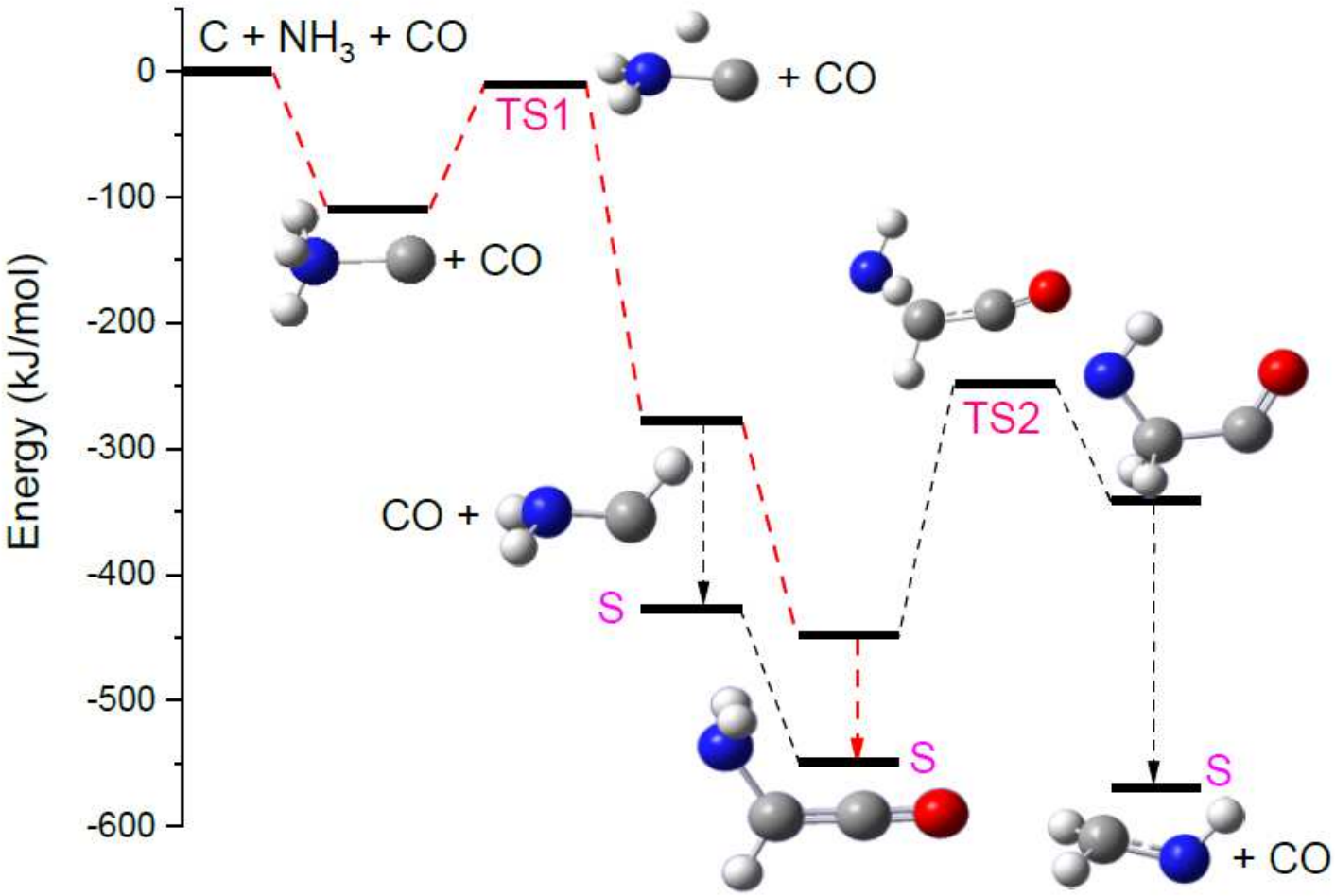

Figure 2

Energy level diagram for the reaction involving CO, C, and NH3 reactants. The reaction starts with the triplet state. The transition states and the singlet states are marked with TS and S, respectively. The dashed lines show the possible reaction pathways and the red colour marks the most probable one.

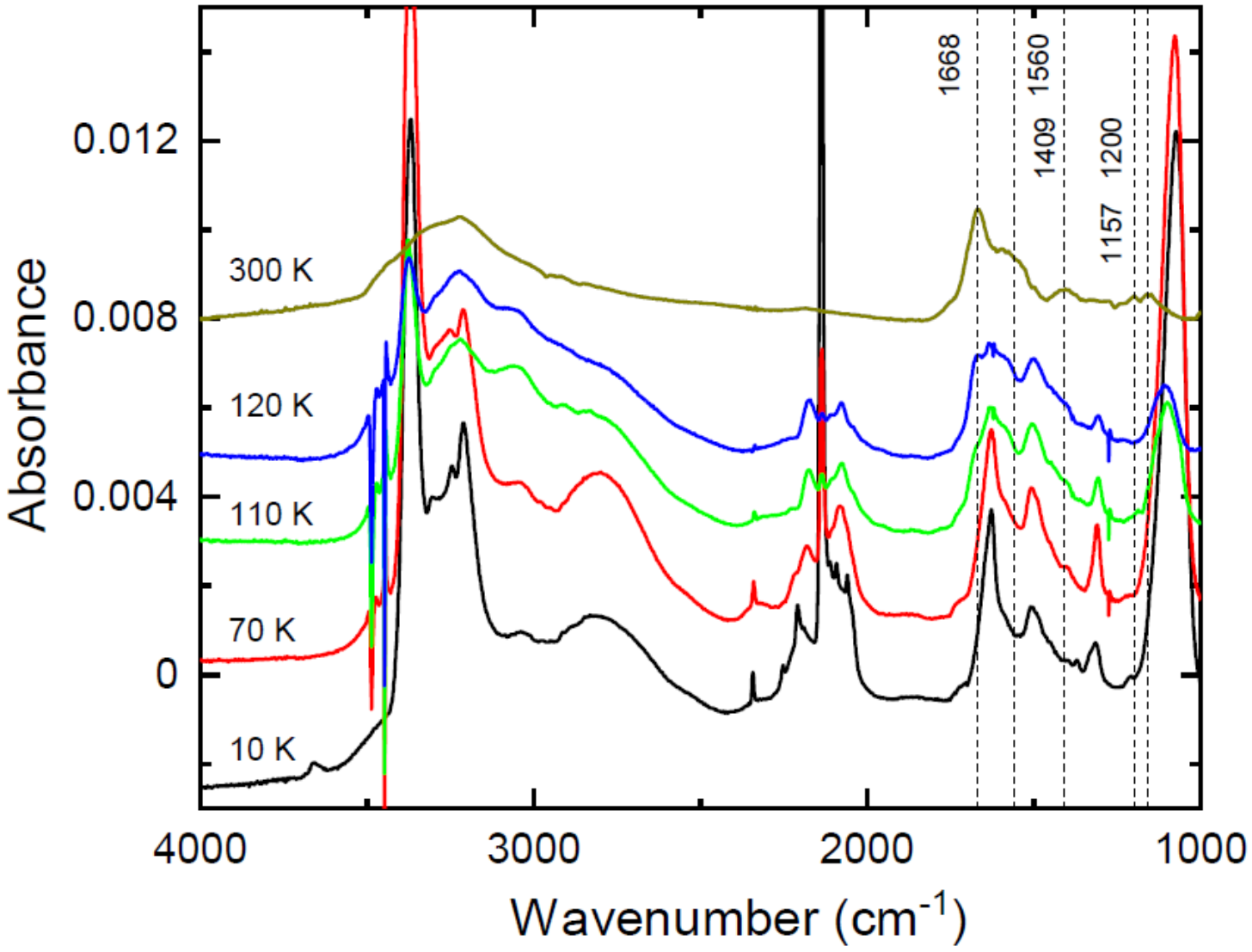

Figure 3

IR absorption spectra during the annealing of the material produced by co-deposition of CO + C + NH3. Vertical numbers show the positions of the peaks appearing during heating, while horizontal ones displays the temperature of the substrate.

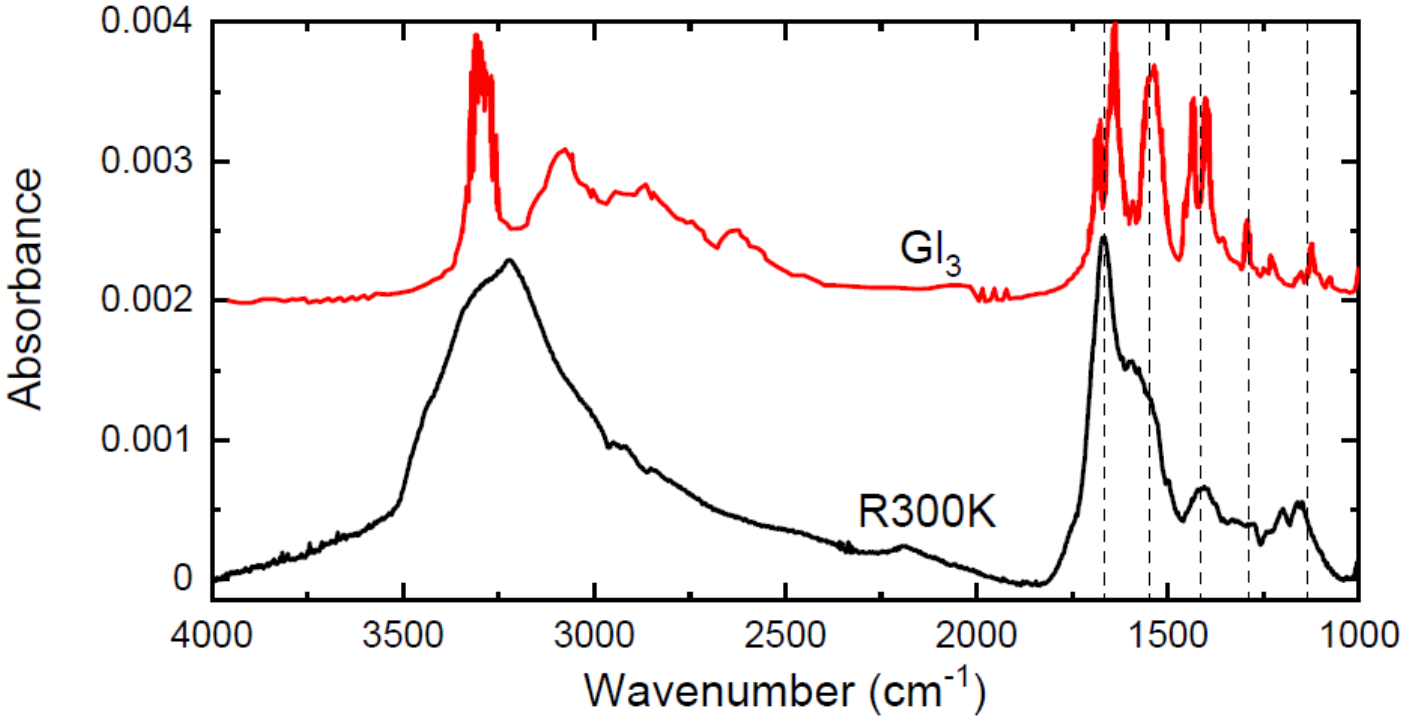

Figure 4

Comparison of the IR absorption spectra of R300K and triglycine (Gl3) adopted from ref 20. The vertical dashed lines are drawn to visualize the coincidences between the peaks in two spectra.

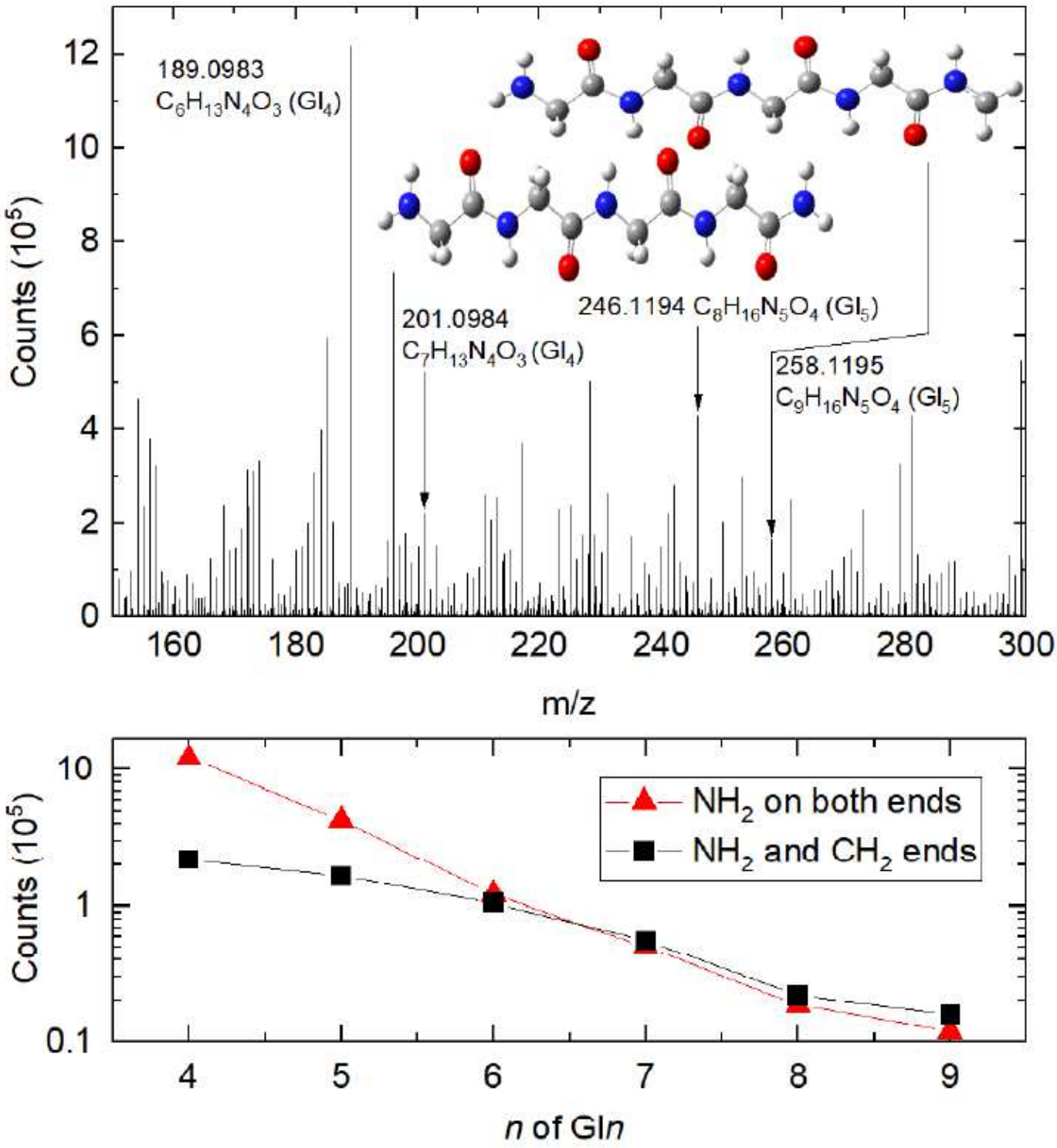

Figure 5

The mass spectra of the 300 K residue obtained from ex situ analysis using ESI-Orbitrap mass spectrometer. The molecular structures displayed resemble the GI5 peptides 138 detected in the mass spectra as protonated species [analyte+H]+. In the lower frame the intensities of the bands from mass spectrum corresponding to the glycine peptides are plotted as a function of the peptide length.

Supplementary Files

This is a list of supplementary files associated with this preprint. Click to download.

- SI.pdf